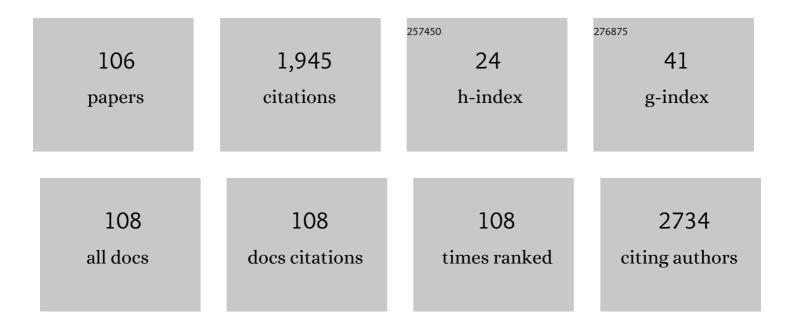
## Dibyendu Bhattacharyya

List of Publications by Year in descending order

Source: https://exaly.com/author-pdf/3188715/publications.pdf Version: 2024-02-01



#	Article	IF	CITATIONS
1	Cu–Cl Thermochemical Water Splitting Cycle: Probing Temperature-Dependent CuCl2 Hydrolysis and Thermolysis Reaction Using In Situ XAS. Journal of Thermal Analysis and Calorimetry, 2022, 147, 7063-7076.	3.6	7
2	CoFeVSb: A promising candidate for spin valve and thermoelectric applications. Physical Review B, 2022, 105, .	3.2	17
3	High-performance aqueous sodium-ion/sulfur battery using elemental sulfur. Journal of Materials Chemistry A, 2022, 10, 11394-11404.	10.3	1
4	Structural properties and luminescence dynamics of CaZrO <sub>3</sub> :Eu <sup>3+</sup> phosphors. Inorganic Chemistry Frontiers, 2021, 8, 821-836.	6.0	24
5	Interface modification of Cr/Ti multilayers with C barrier layer for enhanced reflectivity in the water window regime. Journal of Synchrotron Radiation, 2021, 28, 224-230.	2.4	4
6	Evolution of transition metal charge states in correlation with the structural and magnetic properties in disordered double perovskites Ca <sub>2â^'<i>x</i></sub> La <sub><i>x</i></sub> FeRuO <sub>6</sub> (0.5 ≤i>x ≤2). Physical Chemistry Chemical Physics, 2021, 23, 21769-21783.	2.8	9
7	Role of diluent in the unusual extraction of Am <sup>3+</sup> and Eu <sup>3+</sup> ions with benzene-centered tripodal diglycolamides: local structure studies using luminescence spectroscopy and XAS. New Journal of Chemistry, 2021, 45, 16794-16803.	2.8	2
8	Role of Cobalt Doping in CdS Quantum Dots for Potential Application in Thin Film Optoelectronic Devices. Journal of Physical Chemistry C, 2021, 125, 2074-2088.	3.1	16
9	Insight into the charging–discharging of magnetite electrodes: <i>in situ</i> XAS and DFT study. Physical Chemistry Chemical Physics, 2021, 23, 6051-6061.	2.8	5
10	Two-Dimensional Tungsten Oxide/Selenium Nanocomposite Fabricated for Flexible Supercapacitors with Higher Operational Voltage and Their Charge Storage Mechanism. ACS Applied Materials & Interfaces, 2021, 13, 8102-8119.	8.0	32
11	Identification of a copper ion recognition peptide sequence in the subunit II of cytochrome c oxidase: a combined theoretical and experimental study. Journal of Biological Inorganic Chemistry, 2021, 26, 411-425.	2.6	4
12	Defect persuade paramagnetic properties of nickel doped ZnS nanocrystals and identification of structural, optical, local atomic structure. Journal of Materials Science: Materials in Electronics, 2021, 32, 15563-15576.	2.2	1
13	Local Structural Studies Through EXAFS and Effect of Fe <sup>2+</sup> or Fe <sup>3+</sup> Existence in ZnO Nanoparticles. Journal of Physical Chemistry C, 2021, 125, 13523-13533.	3.1	9
14	Local Structure Investigations of Sequential Sorption of U and Fe on Polyacrylamide Hydroxamic Acid Resins. Inorganic Chemistry, 2021, 60, 10158-10166.	4.0	4
15	An open-access future for <i>Journal of Synchrotron Radiation</i> – Editorial from the Main Editors and IUCr Journals Editor-in-Chief. Journal of Synchrotron Radiation, 2021, 28, 1273-1274.	2.4	1
16	Insights into the Structural and Microscopic Origin of Magnetic Properties of the Î <sup>3</sup> -Fe2O3@MnxOy Nanostructure. Journal of Physical Chemistry C, 2021, 125, 17971-17982.	3.1	7
17	Evolution of the interface microstructure of short-period Cr/Ti multilayers with increase in number of bi-layers. Thin Solid Films, 2021, 734, 138840.	1.8	0
18	Unveiling the genesis of the high catalytic activity in nickel phthalocyanine for electrochemical ammonia synthesis. Journal of Materials Chemistry A, 2021, 9, 14477-14484.	10.3	46

#	Article	IF	CITATIONS
19	Structural, magnetic and electronic properties of Zn0.94Co0.06O/ZnO heterostructure. Applied Physics A: Materials Science and Processing, 2021, 127, 1.	2.3	0
20	Interface evolution of Co/Ti multilayers with ultra-short period. Thin Solid Films, 2020, 693, 137688.	1.8	5
21	Interface evolution of Cr/Ti multilayer films during continuous to discontinuous transition of Cr layer. Vacuum, 2020, 181, 109610.	3.5	7
22	Interplay between local distortion at lattice sites with optical and electrical properties of Eu <sup>3+</sup> -doped MNbO <sub>3</sub> (M = Na and K) compounds. Materials Advances, 2020, 1, 2380-2394.	5.4	20
23	XAS Microstructure Analysis of Manganese Doped Zinc Sulphide Nanophosphor. IEEE Nanotechnology Magazine, 2020, 19, 360-367.	2.0	3
24	<i>In situ</i> modulation of silica-supported MoO <sub>2</sub> /Mo <sub>2</sub> C heterojunction for enhanced hydrogen evolution reaction. Catalysis Science and Technology, 2020, 10, 4776-4785.	4.1	9
25	Exploring functionalized titania for task specific application of efficient separation of trivalent f-block elements. New Journal of Chemistry, 2020, 44, 6151-6162.	2.8	12
26	XAFS study of K-absorption spectra of copper (II) complexes having pentamethyldiethylenetriamine (PMDT) as one of the ligands. AIP Conference Proceedings, 2020, , .	0.4	0
27	Achieving Bright Blue and Red Luminescence in Ca <sub>2</sub> SnO <sub>4</sub> through Defect and Doping Manipulation. Journal of Physical Chemistry C, 2020, 124, 16090-16101.	3.1	16
28	Highly Efficient Extraction of Trivalent f -Cations Using Several N -Pivot Tripodal Diglycolamide Ligands in an Ionic Liquid: The Role of Ligand Structure on Metal Ion Complexation. European Journal of Inorganic Chemistry, 2020, 2020, 191-199.	2.0	6
29	Investigation of New <i>B</i> -Site-Disordered Perovskite Oxide CaLaScRuO <sub>6+δ</sub> : An Efficient Oxygen Bifunctional Electrocatalyst in a Highly Alkaline Medium. ACS Applied Materials & Interfaces, 2020, 12, 9190-9200.	8.0	35
30	Early recrystallization of Ni/Ti multilayer due to disorder in the Ni layer. Journal of Applied Physics, 2020, 127, 165304.	2.5	3
31	Structural studies on transition metal ion complexes of polyethylene oxide-natural rubber block copolymers. Journal of Polymer Research, 2019, 26, 1.	2.4	3
32	First results from the XMCD facility at the Energy-Dispersive EXAFS beamline of the Indus-2 synchrotron source. Journal of Synchrotron Radiation, 2019, 26, 445-449.	2.4	1
33	Investigation of Compression-Induced Deformations in Local Structure and Pore Architecture of ZIF-8 Using FTIR, X-ray Absorption, and Positron Annihilation Spectroscopy. Journal of Physical Chemistry C, 2019, 123, 22273-22280.	3.1	34
34	5-circle diffractometer, mythen 1D detector and TetrAMM picoammeter interfacing in SPEC through EPICS for perform x-ray reflectivity and x-ray absorption measurement at BL-09, Indus-2. AIP Conference Proceedings, 2019, , .	0.4	0
35	Effect of argon-nitrogen mixed ambient Ni sputtering on the interface diffusion of Ni/Ti periodic multilayers and supermirrors. Vacuum, 2019, 169, 108864.	3.5	11
36	Effect of ultrathin Cu buffer layer on interfaces of Co/Ti multilayer for use in water-window region. AIP Conference Proceedings, 2019, , .	0.4	1

#	Article	IF	CITATIONS
37	Interface studies of Mo/Si multilayers with carbon diffusion barrier by grazing incidence extended X-ray absorption fine structure. Thin Solid Films, 2019, 673, 126-135.	1.8	11
38	XANES, EXAFS, EPR, and First-Principles Modeling on Electronic Structure and Ferromagnetism in Mn Doped SnO <sub>2</sub> Quantum Dots. Journal of Physical Chemistry C, 2019, 123, 3067-3075.	3.1	15
39	Structure of copper mixed ligand complex with tetramethylethylenediamine as primary ligand by EXAFS. AIP Conference Proceedings, 2019, , .	0.4	0
40	Magnetically Recoverable Ni/NiO Catalyst for Hydrogenation of Cashew Nut Shell Oil to Value-Added Products. Energy & Fuels, 2019, 33, 5332-5342.	5.1	12
41	Local Structure and Spectroscopic Properties of Eu <sup>3+</sup> -Doped BaZrO <sub>3</sub> . Inorganic Chemistry, 2019, 58, 3073-3089.	4.0	34
42	Operando X-ray absorption spectroscopy study of the Fischer–Tropsch reaction with a Co catalyst. Journal of Synchrotron Radiation, 2019, 26, 137-144.	2.4	7
43	Arsenic surface complexation behavior in aqueous systems onto Al substituted Ni, Co, Mn, and Cu based ferrite nano adsorbents. Journal of Hazardous Materials, 2019, 361, 383-393.	12.4	22
44	Structural investigations on uranium( <scp>vi</scp> ) and thorium( <scp>iv</scp> ) complexation with TBP and DHOA: a spectroscopic study. New Journal of Chemistry, 2018, 42, 5243-5255.	2.8	23
45	Investigating the evolution of local structure around Er and Yb in ZnO:Er and ZnO:Er, Yb on annealing using X-ray absorption spectroscopy. Journal of Applied Physics, 2018, 123, .	2.5	14
46	Deciphering the Role of Charge Compensator in Optical Properties of SrWO <sub>4</sub> :Eu <sup>3+</sup> :A (A = Li <sup>+</sup> , Na <sup>+</sup> , K <sup>+</sup> ): Spectroscopic Insight Using Photoluminescence, Positron Annihilation, and X-ray Absorption. Inorganic Chemistry, 2018, 57, 821-832.	4.0	82
47	Exploring Defect-Induced Emission in ZnAl <sub>2</sub> O <sub>4</sub> : An Exceptional Color-Tunable Phosphor Material with Diverse Lifetimes. Inorganic Chemistry, 2018, 57, 3963-3982.	4.0	72
48	Origin of Local Atomic Order and Disorder in <mml:math xmlns:mml="http://www.w3.org/1998/Math/MathML" display="inline" overflow="scroll"&gt;<mml:msub><mml:mi>Co</mml:mi><mml:mn>2</mml:mn></mml:msub><mml:msub><mml:r Heusler Alloys: Theory and Experiment. Physical Review Applied, 2018, 10, .</mml:r </mml:msub></mml:math 	ni <sup>3</sup> Fe <td>nl:mi&gt;<mml:< td=""></mml:<></td>	nl:mi> <mml:< td=""></mml:<>
49	Probing local structures in (Ni/Co)â€codoped ZnO/PVDF composite flexible and freestanding films by using XAS and XPS studies. X-Ray Spectrometry, 2018, 47, 484-494.	1.4	2
50	First Report on the Complexation of Actinides and Lanthanides Using 2,2′,2′′-(((1,4,7-Triazonane-1,4,7-triyl)tris(2-oxoethane-2,1-diyl)) tris(oxy)) tris( <i>N</i> , <i>N</i> -dioctylacetamide): Synthesis, Extraction, Luminescence, EXAFS, and DFT Studies. Inorganic Chemistry, 2018, 57, 12987-12998.	4.0	23
51	2D and 3D Silicaâ€Templateâ€Derived MnO <sub>2</sub> Electrocatalysts towards Enhanced Oxygen Evolution and Oxygen Reduction Activity. ChemElectroChem, 2018, 5, 3980-3990.	3.4	35
52	Morphology, Stability, Structure, and CO <sub>2</sub> –Surface Chemistry of Micelle Nanolithographically Prepared Two-Dimensional Arrays of Core–Shell Fe–Pd Multicomponent Nanoparticles. Journal of Physical Chemistry C, 2018, 122, 26528-26542.	3.1	1
53	Effect of ionic size compensation by Ag+ incorporation in homogeneous Fe-substituted ZnO: studies on structural, mechanical, optical, and magnetic properties. RSC Advances, 2018, 8, 24355-24369.	3.6	14
54	Selective Oxidation of Cyclohexane to Cyclohexanone Using Chromium Oxide Supported Mesoporous MCMâ€41 Nanospheres: Probing the Nature of Catalytically Active Chromium Sites. ChemCatChem, 2018, 10. 3291-3298.	3.7	15

#	Article	IF	CITATIONS
55	In Situ XAS Study on Growth of PVPâ€Stabilized Cu Nanoparticles. ChemistrySelect, 2018, 3, 7370-7377.	1.5	7
56	Structural Investigations of (Ni,Cu) Co–Doped ZnO Nanocrystals by Xâ€ray Absorption Spectroscopy. ChemistrySelect, 2018, 3, 5644-5651.	1.5	4
57	Search for Origin of Room Temperature Ferromagnetism Properties in Ni-Doped ZnO Nanostructure. ACS Applied Materials & Interfaces, 2017, 9, 7691-7700.	8.0	99
58	Insight into growth of Au–Pt bimetallic nanoparticles: an <i>inÂsitu</i> XAS study. Journal of Synchrotron Radiation, 2017, 24, 825-835.	2.4	12
59	Manifestation of Concealed Defects in MoS2Nanospheres for Efficient and Durable Electrocatalytic Hydrogen Evolution Reaction. ChemistrySelect, 2017, 2, 4667-4672.	1.5	2
60	The Magnetic Properties of Sol-Gel Synthesized TM <sub>0.03</sub> Zn <sub>0.97</sub> O (TM: Mn, Fe,) Tj ETG	2q0 <u>0</u> 9 rg	BT <u>{</u> Overlock
61	Nano-structured hybrid molybdenum carbides/nitrides generated in situ for HER applications. Journal of Materials Chemistry A, 2017, 5, 7764-7768.	10.3	64
62	Origin of Blue-Green Emission in α-Zn <sub>2</sub> P <sub>2</sub> O <sub>7</sub> and Local Structure of Ln <sup>3+</sup> Ion in α-Zn <sub>2</sub> P <sub>2</sub> O <sub>7</sub> :Ln <sup>3+</sup> (Ln = Sm,) Tj 167-178.	ETQq0 0 0	) rgBT /Overlc
63	Graphene Quantum Dot Solid Sheets: Strong blue-light-emitting & photocurrent-producing band-gap-opened nanostructures. Scientific Reports, 2017, 7, 10850.	3.3	61
64	Development and characterization of soft X-ray synchrotron mirror. AIP Conference Proceedings, 2017, , .	0.4	0
65	Local Structure Investigation of Mn―and Co–Doped TiO <sub>2</sub> Thin Films by Xâ€Ray Absorption Spectroscopy. ChemistrySelect, 2017, 2, 11012-11024.	1.5	5
66	Phase transformation of [Co/Ti]x10 multilayer under swift heavy ion irradiation. Journal of Applied Physics, 2017, 122, 025302.	2.5	2
67	Flow-setup for in situ XAFS measurement to probe growth of PVP stabilized Cu nanoparticles. AIP Conference Proceedings, 2017, , .	0.4	1
68	Structural, electronic, magnetic, and transport properties of the equiatomic quaternary Heusler alloy CoRhMnGe: Theory and experiment. Physical Review B, 2017, 96, .	3.2	54
69	Ti K-edge X-ray absorption spectra of spray pyrolysis synthesized TiO2-x and TiO2-x Nx thin films. AIP Conference Proceedings, 2017, , .	0.4	0
70	Investigation of band alignment in Co doped ZnO/ZnO heterostructure. AIP Conference Proceedings, 2017, , .	0.4	0
71	Structural investigations of (Mn, Dy) co-doped ZnO nanocrystals using X-ray absorption studies. RSC Advances, 2017, 7, 56662-56675.	3.6	25
72	Performance of Co/Ti multilayers in a water window soft x-ray regime. Applied Optics, 2017, 56, 7525.	1.8	8

#	Article	IF	CITATIONS
73	Local structure investigation of Co doped ZnO thin films prepared by RF sputtering technique. AlP Conference Proceedings, 2016, , .	0.4	0
74	Growth of Au@Pt coreshell nanoparticles: Probed by in-situ XANES and UV-visible spectroscopy. AIP Conference Proceedings, 2016, , .	0.4	0
75	Local structure studies of Ni doped ZnO/PVDF composite free-standing flexible thin films using XPS and EXAFS studies. Journal of Polymer Research, 2016, 23, 1.	2.4	8
76	Size-Induced Structural Phase Transition at â^¼6.0 nm from Mixed fcc–hcp to Purely fcc Structure in Monodispersed Nickel Nanoparticles. Journal of Physical Chemistry C, 2016, 120, 28354-28362.	3.1	26
77	EXAFS measurements on Mn doped CaF2 phosphor with different Mn concentrations. AIP Conference Proceedings, 2016, , .	0.4	0
78	Effect of gamma irradiation on X-ray absorption andÂphotoelectron spectroscopy of Nd-doped phosphate glass. Journal of Synchrotron Radiation, 2016, 23, 1424-1432.	2.4	14
79	CO oxidation activity enhancement of Ce <sub>0.95</sub> Cu <sub>0.05</sub> O <sub>2â<sup>^</sup>î</sub> induced by Pd co-substitution. Catalysis Science and Technology, 2016, 6, 8104-8116.	4.1	16
80	Investigation of Fe doped ZnO thin films by X-ray absorption spectroscopy. RSC Advances, 2016, 6, 74982-74990.	3.6	27
81	Nitrogen Doping in Oxygen-Deficient Ca <sub>2</sub> Fe <sub>2</sub> O <sub>5</sub> : A Strategy for Efficient Oxygen Reduction Oxide Catalysts. ACS Applied Materials & Interfaces, 2016, 8, 34387-34395.	8.0	46
82	Augmentation of the step-by-step Energy-Scanning EXAFS beamline BL-09 to continuous-scan EXAFS mode at INDUS-2 SRS. Journal of Synchrotron Radiation, 2016, 23, 1518-1525.	2.4	20
83	Investigation of gamma radiation induced changes in local structure of borosilicate glass by TDPAC and EXAFS. Hyperfine Interactions, 2016, 237, 1.	0.5	5
84	Structural and optical properties of sol–gel derived Cr-doped ZnO diluted magnetic semiconductor nanocrystals: an EXAFS study to relate the local structure. RSC Advances, 2016, 6, 107816-107828.	3.6	33
85	Variation of local atomic structure due to devitrification of Ni-Zr alloy thin films probed by EXAFS measurements. AIP Conference Proceedings, 2016, , .	0.4	0
86	Luminescence Properties of SrZrO <sub>3</sub> /Tb <sup>3+</sup> Perovskite: Host-Dopant Energy-Transfer Dynamics and Local Structure of Tb <sup>3+</sup> . Inorganic Chemistry, 2016, 55, 1728-1740.	4.0	96
87	Unique selectivity reversal in Am <sup>3+</sup> –Eu <sup>3+</sup> extraction in a tripodal TREN-based diglycolamide in ionic liquid: extraction, luminescence, complexation and structural studies. Dalton Transactions, 2016, 45, 2476-2484.	3.3	61
88	X-ray absorption spectroscopy of Mn doped ZnO thin films prepared by rf sputtering technique. AIP Advances, 2015, 5, 117138.	1.3	21
89	Optical and local structural study of Gd doped ZrO2 thin films deposited by RF magnetron sputtering technique. AIP Conference Proceedings, 2015, , .	0.4	3
90	X-ray absorption studies of gamma irradiated Nd doped phosphate glass. AIP Conference Proceedings, 2015, , .	0.4	5

#	Article	IF	CITATIONS
91	First phase commissioning of high pressure XAFS setup at ED-XAFS beamline, Indus-2 synchrotron radiation source, India. Journal of Optics (India), 2015, 44, 182-194.	1.7	1
92	Spectroscopic investigations on sorption of uranium onto suspended bentonite: effects of pH, ionic strength and complexing anions. Radiochimica Acta, 2015, 103, 293-303.	1.2	4
93	Correlation of Mo dopant and photocatalytic properties of Mo incorporated TiO <sub>2</sub> : an EXAFS and photocatalytic study. RSC Advances, 2015, 5, 90932-90940.	3.6	16
94	Nitrogen Location and Ti–O Bond Distances in Pristine and N-Doped TiO <sub>2</sub> Anatase Thin Films by X-ray Absorption Studies. Journal of Physical Chemistry C, 2015, 119, 17640-17647.	3.1	40
95	An insight into local environment of lanthanide ions in Sr <sub>2</sub> SiO <sub>4</sub> :Ln (Ln = Sm,) Tj ETQq1	1 0 78431 2.8	L4 <sub>32</sub> BT /Ove
96	Physiochemical Investigation of Shape-Designed MnO <sub>2</sub> Nanostructures and Their Influence on Oxygen Reduction Reaction Activity in Alkaline Solution. Journal of Physical Chemistry C, 2015, 119, 6604-6618.	3.1	106
97	A comprehensive facility for EXAFS measurements at the INDUS-2 synchrotron source at RRCAT, Indore, India. Journal of Physics: Conference Series, 2014, 493, 012032.	0.4	146
98	Cation distribution in Nilâ^'xZnxFe2O4 using X-ray absorption spectroscopy. , 2014, , .		1
99	Study of optical properties of asymmetric bipolar pulse DC magnetron sputtered Ta2O5 thin film as a function of oxygen content in deposition ambient. , 2014, , .		1
100	Installation and commissioning of a large area coating system for neutron and X-ray optical devices. , 2014, , .		1
101	Design and development of an in-line sputtering system and process development of thin film multilayer neutron supermirrors. Review of Scientific Instruments, 2014, 85, 123103.	1.3	14
102	Nature of WO4 tetrahedra in blue light emitting CaWO4 probed through the EXAFS technique. RSC Advances, 2014, 4, 15606.	3.6	15
103	EXAFS study on yttrium oxide thin films deposited by RF plasma enhanced MOCVD under the influence of varying RF self-bias. Applied Surface Science, 2014, 314, 400-407.	6.1	4
104	Correlation of interface roughness for ion beam sputter deposited W/Si multilayers. Journal of Applied Physics, 2011, 109, 084311.	2.5	16
105	Supported Rh2O3 sub-nanometer size particles for direct amination of ethylene with piperidine. Catalysis Science and Technology, 0, , .	4.1	0
106	Structures of Iron-Lithium-Calcium-Silicate Glass and its Devitrified State. Silicon, 0, , 1.	3.3	0